Atomic scale protection using fullerene encapsulation

B. N. Cotier, M. D. Upward, F. H. Jones, P. Moriarty, and P. H. Beton

Atomic scale protection using fullerene encapsulation

B. N. Cotier, M. D. Upward, F. H. Jones, P. Moriarty, and P. H. Beton[a)]
School of Physics and Astronomy, University of Nottingham, University Park, Nottingham NG7 2RD, United Kingdom

The use of fullerene multilayers as a removable protective coating on a clean, reconstructed semiconductor surface has been investigated using an ultrahigh vacuum scanning tunneling microscope (UHV-STM). We have found that the Ag/Si(111)-$\sqrt{3} \times \sqrt{3}$R30° surface, which is normally stable only under an UHV environment, can survive exposure to ambient conditions beneath a protective layer of C_{60}. The C_{60} capping layer may be removed by annealing after reinsertion into UHV. For optimum protection a thickness >5 monolayers is required. The protective effect lasts for times of order several minutes. © *2001 American Institute of Physics.*
[DOI: 10.1063/1.1336553]

The development of molecular scale analogs of macroscopic processes forms an important part of the growing field of nanometer scale science and technology. Patterning of surfaces and the assembly of simple structures on the atomic and molecular scale have been widely demonstrated[1–4] and in this letter we address a related problem concerning the protection of atomic and molecular scale nanostructures from degradation through exposure to ambient conditions. This is particularly relevant for structures which are fabricated under vacuum conditions. For macroscopic materials, protection is routinely achieved through encapsulation of a surface or material of interest in an unreactive coating. However it is not clear that an analogous approach will be viable for the atomic scale protection of, for example, a clean surface. To achieve this objective the protective coating should interact sufficiently weakly with the surface so that modification through the formation of chemical bonds is avoided, while simultaneously inhibiting atmospheric attack. Note that many of the procedures for passivation of clean surfaces, for example H passivation of Si(100)-2×1, rely on chemical modification of the surface.[5] Similarly, the use of fullerenes as protective coatings on Si(111)-7×7 has been investigated[6–9] and results in the formation of strong chemical bonds.[9] Consequently, while such films inhibit the oxidation of the underlying Si surface,[9] the interfacial fullerene monolayer cannot be completely removed.[6]

In this letter we describe the use of C_{60} as a protective coating on the Ag/Si(111)-$\sqrt{3} \times \sqrt{3}$R30° surface, hereafter referred to as Ag/Si. Coated surfaces are exposed to atmospheric conditions and, upon removal of the C_{60} layers under ultrahigh vacuum (UHV), large areas of the Ag/Si surface are found to survive with atomic scale integrity. We find that the effectiveness of the protection layer is related to the morphology of the underlying Ag/Si and for short exposure times is independent of the number of deposited layers above a critical thickness.

Samples of size 7 mm×3 mm were cut from *p*-type B-doped Si(111) wafers ($\rho \sim 1 \Omega$ cm) and loaded into an UHV chamber (base pressure $\sim 10^{-10}$ Torr). After degassing

overnight at 650 °C the sample was flash annealed at ~ 1200 °C for ~ 1 min to create the clean Si(111)-7×7 surface. To form the Ag/Si(111)-$\sqrt{3} \times \sqrt{3}$R30° reconstruction Ag was deposited on the Si(111)-7×7 surface (sample held at ~ 550 °C).[10–12] C_{60} was deposited onto the Ag/Si surface from a Knudsen cell (deposition rate ~ 0.75 monolayers/min; sample at room temperature). Samples were exposed to atmospheric conditions by removing the sample holder from the UHV chamber. After exposure the sample was reintroduced into UHV conditions. This sequence of steps took ~ 5 min to perform and the minimum period of time in which the sample was exposed to ambient conditions was ~ 20 s. The sample was then annealed at ~ 350 °C to remove the C_{60}.[13] Images of the surface were acquired using a scanning tunneling microscope (STM) operated in constant current mode at room temperature. Electrochemically etched tungsten (W) tips which were cleaned in UHV by electron beam bombardment from a hot W filament were used for STM imaging.

Figure 1(a) is a STM image of the Ag/Si surface, in which Ag atoms appear as bright features.[10–12] All surface dangling bonds, apart from those present at step edges and defects, are passivated through the formation of Ag–Si bonds, leaving the surface relatively unreactive. Nevertheless the surface is still sufficiently reactive to be corrupted completely by exposure to ambient conditions [see Fig. 1(b)] which shows a Ag/Si sample after exposure to the atmosphere for ~ 20 s. There is no evidence in this image for the atomic scale features observed in Fig. 1(a).

Figure 1(c) shows a Ag/Si surface following the deposition of ~ 5 monolayers (ML) of C_{60}. Highly ordered, hexagonally packed islands of C_{60} (typical island width ~ 20 nm) are formed with principal axes oriented ±11° to the $\langle 1, 1, -2 \rangle$ direction of the Si surface.[13,14] Several discrete contrast levels are evident in Fig. 1(c), corresponding to different C_{60} terraces. C_{60} islands are nucleated at step edges and other defects (for example domain boundaries[13]) on the Ag/Si surface. These defects thus determine the morphology of C_{60} multilayers.

Following multilayer deposition the surface is exposed to atmosphere for 20 s as described above. After reentry into UHV C_{60} is removed by annealing at ~ 350 °C. For control
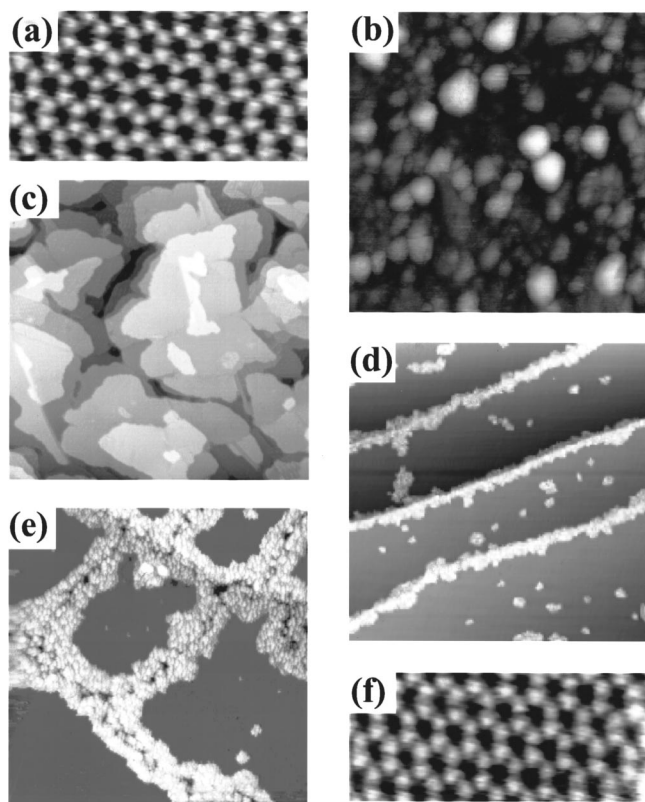
[a)]Electronic mail: peter.beton@nottingham.ac.uk

FIG. 1. (a) STM image (8 nm×3.5 nm; −1.2 V, −0.3 nA) of the clean reconstructed Ag/Si(111)−($\sqrt{3} \times \sqrt{3}$)R30° surface; (b) image (100 nm ×100 nm; 2.5 V, 0.2 nA) showing corrupted surface immediately after ~20 s exposure to air; (c) image (120 nm×120 nm; −3 V, −0.3 nA) showing Ag/Si(111)−($\sqrt{3} \times \sqrt{3}$)R30° surface covered with ~5 ML of C_{60}. Brightest areas correspond to highest layer islands; (d) image (120 nm×120 nm; 2 V, 0.2 nA) showing C_{60} bound to step edges and defects present on terraces. Bright areas represent C_{60} molecules; (e) image (100 nm×100 nm; −2.5 V, −0.2 nA) showing Ag/Si after ~20 s exposure to air and removal of C_{60} layers by annealing; (f) image (8 nm×3 nm; −1.2 V, −0.5 nA) showing that Ag/Si(111)−($\sqrt{3} \times \sqrt{3}$)R30° surface survives exposure.

purposes we show an image [Fig. 1(d)] taken after annealing of a sample which was not removed from UHV. As shown in Fig. 1(d) C_{60} remains bound to dangling bonds at step edges, domain boundaries and terrace defects, but most of the surface (~80%) is still terminated by the Ag/Si reconstruction. Figure 1(e) shows a Ag/Si sample that has been exposed to air for ~20 s prior to annealing.

A comparison of Figs. 1(d) and 1(e) shows that exposure of the sample to atmosphere increases the fraction of the surface area which is corrupted. It is also evident from Fig. 1(e) that the corruption has proceeded through an increase in the width of the quasilinear regions which follow step edges and domain boundaries. In Fig. 1(d) the width of these regions is ~6 nm, while in Fig. 1(e) it is ~12 nm. However within the areas enclosed by the network of corrupted regions of the Ag/Si reconstruction is preserved on the terraces. This is shown clearly in Fig. 1(f) which corresponds to a high magnification image of the darker (lower) regions in Fig. 1(e) and has the same atomic scale features as observed in Fig. 1(a). In addition the uncorrupted regions have areas of the same order of magnitude as the C_{60} islands shown in Fig. 1 and it is likely that the corruption is initiated at the base of these islands where the protective film is thinner and less ordered.
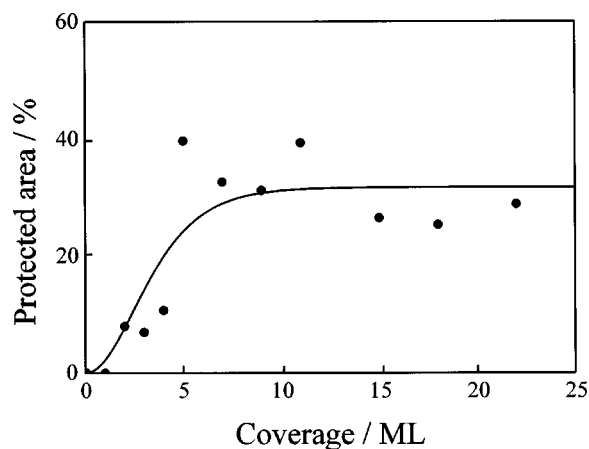

FIG. 2. Dependence of protective effect on film thickness for fixed ~20 s exposure time. The curve is intended as a guide for the eye.

This procedure has been repeated for C_{60} films of varying thickness and the fraction of the area which remains protected is plotted as a function of film thickness in Fig. 2. These data show clearly that there is a threshold coverage of ~5 ML below which the protection is ineffective. At higher coverage 35%–40% of the sample is effectively protected (however note that even for the sample which was not exposed to atmosphere only 80% of the sample surface is recovered as clean Ag/Si). As stated above for these short exposure times corruption is associated with step edges and domain boundaries on the Ag/Si surface. The variability of the reconstructed surface from sample to sample accounts for the spread in the fractional protection above the threshold of 5 ML.

We have also investigated the dependence of the protective effect upon exposure time, for a fixed C_{60} coverage, ~15 ML. Figure 3 shows a plot of the fraction of uncorrupted area versus exposure time, t. It is evident from these data that the corrupted area increases with exposure time, and for the coverage used, the sample has a lifetime of ~5–10 min in air before complete corruption occurs. In addition the time dependence provides evidence that two distinct modes of corruption are active, since the rate of change of the fractional coverage with time (on a logarithmic scale) shows a discontinuity at a time ~2 min. For short times the fractional area, F, which has been protected has a time dependence given by
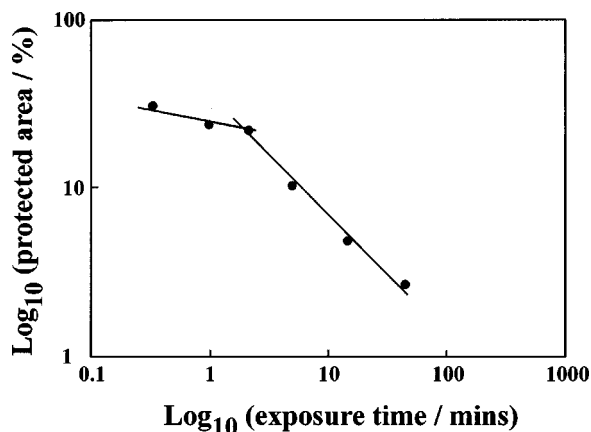

FIG. 3. Dependence of protective effect upon exposure time for fixed (15 ML) coverage.

$F \alpha t^{-0.15}$. Above this time the corruption is much more rapid, $F \alpha t^{-0.78}$. STM images following removal of C_{60} for long exposure times show that many localized corrupted regions appear on the surface indicating that the penetration of atmospheric constituents on this time scale proceeds via diffusion through the thickest parts of the film rather than progressive ingress from the edges of the islands where the initial corruption is concentrated.

Overall these results may be understood if we consider the alternative diffusion paths through the protective film. Atmospheric contaminants may either diffuse through the thinnest parts of the film at the edges of the ordered islands or through the thicker regions of the film. Our results imply that atmospheric oxygen diffuses through the thinner regions at the edges of the C_{60} islands on a time scale which is fast compared to our minimum measurement time giving rise to surfaces such as Fig. 1(d). For the thinner films (<5 ML) diffusion to the C_{60}–Ag/Si interface is also possible for these short times. However, for the thicker films further corruption proceeds by diffusion directly through the thicker film. Evidence for this is provided by an increase in isolated corrupted regions within the type of network shown in Fig. 1(e). This would imply that a time of order 2 min is required for diffusion through films with thickness of order 10 ML. The influence of oxygen diffusion on the conductivity of fullerene films has been investigated previously.[15,16] The conductivity of thick C_{60} films reduces on a time scale of order minutes when exposed to a partial pressure of O_2. While it is difficult to compare this work directly with our observations we note that the order of magnitudes of these results are consistent.

In conclusion, we have investigated the use of C_{60} layers as a protective coating. The degree of protection provided by the coating is dependent on film thickness but is strongly influenced by the morphology of the initial surface. The protective effect persists for $\sim$5–10 min in air, which is sufficient to permit the transport of fragile samples, for example metallic nanowires, through the atmosphere. Overall, this work describes a general technique for protecting atomically clean samples against contamination in air. We propose that this method could be applied to other systems where there is a similarly weak adsorbate–substrate interaction, allowing simple deposition and removal of the protective layers as required.

[1] R. S. Becker, Y. J. Chabal, G. S. Higashi, and A. J. Becker, Phys. Rev. Lett. **65**, 1917 (1990).
[2] D. M. Eigler and E. K. Schweizer, Nature (London) **344**, 524 (1990).
[3] J. W. Lydling, T. C. Shen, J. S. Hubcek, J. R. Tucker, and G. C. Abeln, Appl. Phys. Lett. **64**, 2010 (1994); T. C. Shen, C. Wang, G. C. Abeln, J. R. Tucker, J. W. Lyding, P. Avouris, and R. E. Walkup, Science **268**, 1590 (1995).
[4] P. H. Beton, A. W. Dunn, and P. Moriarty, Appl. Phys. Lett. **67**, 1075 (1995); P. Moriarty, Y.-R. Ma, M. D. Upward, and P. H. Beton, Surf. Sci. **407**, 27 (1998).
[5] J. J. Boland, Surf. Sci. **261**, 17 (1992).
[6] A. W. Dunn, P. Moriarty, M. D. Upward, and P. H. Beton, Appl. Phys. Lett. **69**, 506 (1996).
[7] H. Hong, W. E. McMahon, P. Zschack, D.-S. Lin, R. D. Aburano, H. Chen, and T-C. Chiang, Appl. Phys. Lett. **61**, 3127 (1992).
[8] A. V. Hamza, J. Dykes, W. D. Moseley, L. Dinh, and M. Balooch, Surf. Sci. **318**, 368 (1994).
[9] P. Moriarty, M. D. Upward, A. W. Dunn, Y.-R. Ma, P. H. Beton, and D. Teehan, Phys. Rev. B **57**, 362 (1998).
[10] T. Takahashi, S. Nakatani, N. Okamoto, T. Ichikawa, and S. Kikuta, Jpn. J. Appl. Phys., Part 2 **27**, L753 (1988).
[11] D. W. McComb, R. A. Wolkow, and P. A. Hackett, Phys. Rev. B **50**, 18268 (1994).
[12] T. Nakayama, S. Watanabe, and M. Aono, Surf. Sci. **344**, 143 (1995).
[13] M. D. Upward, P. Moriarty, and P. H. Beton, Phys. Rev. B **56**, R1704 (1997).
[14] T. Nakayama, J. Onoe, K. Takeuchi, and M. Aono, Phys. Rev. B **59**, 12627 (1999).
[15] A. Hamed, Y. Y. Sun, Y. K. Tao, R. L. Meng, and P. H. Hor, Phys. Rev. B **47**, 10873 (1993).
[16] T. Arai, Y. Murakami, H. Suematsu, K. Kikuchi, Y. Achiba, and I. Ikemoto, Solid State Commun. **84**, 827 (1992).